Parametric Study of Equivalent Homogeneous Earth Method for Overhead Lines Above A Multi-Layer Earth

H. Xue, J. Mahseredjian, J. Morales, I. Kocar and A. Xémard

***Abstract*--This paper presents a systematic investigation of equivalent homogeneous earth method (EHEM) for calculation of earth-return impedance of overhead conductors above a multi-layer earth. The recently developed EHEM is based on the concept of equivalent propagation constant of earth. The characteristics of equivalent propagation constant of earth and integrand convergences of EHEM are further studied. The parametric studies of accuracy on earth-return impedance between exact formula (EF) and EHEM are also presented in this paper.**

***Keywords*: Earth-return parameters, overhead lines, equivalent homogeneous earth method, frequency domain study, multi-layer earth.**

I. Introduction

SURGE analysis in power transmission systems requires accurate calculations of earth-return parameters. Earth-return impedance and admittance are significantly influenced by the characteristics of earth compositions [1]. In reality, the earth has a layered structure and generally consists of three to five layers [2]-[15] with different electromagnetic properties. Also, several formulations of earth-return impedance on overhead lines are proposed in [2]-[15].

Recently, an Equivalent Homogeneous Earth Method (EHEM) that calculates the earth-return impedance and admittance of overhead lines above an *N*-layer earth was developed in [16], [17]. The EHEM adopts a newly proposed concept of equivalent propagation constant of earth, thus the EHEM can deal with arbitrary earth electromagnetic properties. In comparison to the exact formula (EF), for which more details can be found in [17], the EHEM has several remarkable advantages, such as high accuracy, simplification of formulas and high computational efficiency [17].

Although EHEM is well derived in [15]-[17], several significant aspects i.e., equivalent propagation constant of earth, convergence characteristics of integrand used in EHEM and parametric study of EHEM, still need further investigations in comparison to EF method in frequency domain.

Therefore, this paper presents research work regarding further validation of EHEM proposed in [17]. The paper is organized by the following sections. In Section II, the theoretical backgrounds of EHEM and EF methods are reviewed and summarized. In Section III - A, since the newly produced EHEM is based on the equivalent propagation constant of earth, the characteristics of equivalent propagation constant of earth are studied by adopting different real multi-layer earth compositions. Also, the convergences of integrand used in EHEM and EF methods are discussed and compared based on various conditions in Section III - B. Moreover, the parametric influences on the deviations of self- and mutual earth-return impedances calculated using EHEM and EF methods are investigated in Section III - C. It gives solid validations for EHEM, which have not been performed in [17].

II. Theoretical Background

Fig. 1 shows a transmission system composed of overhead conductors above an *N*-layer earth. The radii of conductor *i* and *j* are r_i and r_j. The term d represents depth of earth layer and the depth of the lowest layer extends to infinity.

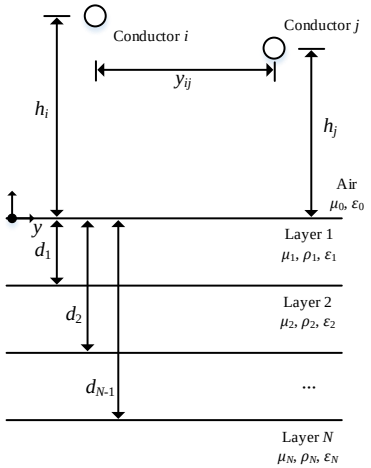

Fig. 1 Overhead conductors above an *N*-layer earth.

The permeability and permittivity of air are set to μ_0 and ε_0. The permeability, resistivity and permittivity of the *N*-layer earth are defined by μ_n, ρ_n (conductivity $\sigma_n = 1/\rho_n$) and ε_n, where $n = 1 \cdots N$. The conductor heights are h_i

H. Xue and J. Mahseredjian are with Polytechnique Montréal, Canada (e-mails: haoyan.xue@polymtl.ca, jeanm@polymtl.ca).
J. Morales is with PGSTech, Canada (e-mail jesus.morales@emtp.com).
I. Kocar is with Hong Kong Polytechnic University, Hongkong (email: ilhan.kocar@polyu.edu.hk).
A. Xémard is with EDF, France (email: alain.xemard@edf.fr).

Paper submitted to the International Conference on Power Systems Transients (IPST2023) in Thessaloniki, Greece, June 12-15, 2023.

and h_j, and y_{ij} represents the horizontal distance between two conductors.

A. Calculation of series impedance of overhead lines

The transmission line (TL) based approach can be characterized by the extended and classical TL methods [18]-[26]. For the extended TL approach, the generalized formula of series impedance of a multi-phase overhead line shown in Fig. 1 has the following expressions [18]-[26].

$$\mathbf{Z} = \mathbf{Z_i} + \mathbf{Z_e} \tag{1}$$

where $\mathbf{Z_i}$ is an internal impedance matrix and $\mathbf{Z_e}$ is an earth-return impedance matrix.

The diagonal element of matrix $\mathbf{Z_i}$ can be evaluated using various formulas proposed in [1], [27].

B. Expressions of earth-return impedance

The mutual element of $\mathbf{Z_e}$ in (1) can be calculated by the following expression [17].

$$Z_{eij} = \frac{j\omega\mu_0}{2\pi}\ln\left(\frac{D_2}{D_1}\right) + \Delta Z_{eij} \tag{2}$$

where

$$D_1 = \sqrt{y_{ij}^2 + \left(h_i - h_j\right)^2}\,, \quad D_2 = \sqrt{y_{ij}^2 + \left(h_i + h_j\right)^2} \tag{3}$$

The term ΔZ_{eij} represents the correction of lossy earth with stratified structure of soil up to N layers, and it has

$$\Delta Z_{eij} = \frac{j\omega\mu_0}{\pi}\int_0^{+\infty} F(s)\,e^{-s\left(h_i+h_j\right)}\cos\left(sy_{ij}\right)ds \tag{4}$$

The exact formula of irrational $F(s)$ in (4) has been derived in reference [17] based on a recursive method, and it gives

$$F_{\mathrm{EF}}(s) = \frac{F_{G(1)}(s) + F_{T(1)}(s)}{\left(s+\mu_0 b_1\right)F_{G(1)}(s) + \left(s-\mu_0 b_1\right)F_{T(1)}(s)} \tag{5}$$

with

$$F_{G(N-1)}(s) = b_{N-1} + b_N$$

$$F_{T(N-1)}(s) = \left(b_{N-1} - b_N\right)e^{-2a_{N-1}d_{N-1}}$$

$$\vdots$$

$$F_{G(m)}(s) =$$

$$\left(b_m + b_{m+1}\right)F_{G(m+1)}(s) + \left(b_m - b_{m+1}\right)F_{T(m+1)}(s)e^{2a_{m+1}d_m}$$

$$F_{T(m)}(s) = \Big[\left(b_m - b_{m+1}\right)F_{G(m+1)}(s)$$

$$+\left(b_m + b_{m+1}\right)F_{T(m+1)}(s)e^{2a_{m+1}d_m}\Big]e^{-2a_m d_m} \tag{6}$$

and

$$a_n = \sqrt{s^2 + \gamma_n^2 - \gamma_0^2}\,, \quad b_n = a_n/\mu_n\,, \quad d_m = d_1\cdots d_{N-2} \tag{7}$$

$$\gamma_0^2 = j\omega\mu_0 j\omega\varepsilon_0\,, \quad \gamma_n^2 = j\omega\mu_n\left(\sigma_n + j\omega\varepsilon_n\right), \quad 1 \le m \le N-2 \tag{8}$$

Recently, the EHEM based $F(s)$ in (4) has been proposed and developed in reference [17]. Considering an N-layer earth structure, it has the following formula.

$$F_{\mathrm{EHEM}}(s) = \frac{1}{s + \sqrt{s^2 + \gamma_{eq}^2}} \tag{9}$$

where the equivalent propagation constant of N-layer earth has

$$\gamma_{eq} = \gamma_{e1}\frac{\gamma_{e1} + \gamma_{eq2,3} - \left(\gamma_{e1} - \gamma_{eq2,3}\right)e^{-2|d_1|\gamma_{e1}}}{\gamma_{e1} + \gamma_{eq2,3} + \left(\gamma_{e1} - \gamma_{eq2,3}\right)e^{-2|d_1|\gamma_{e1}}} \tag{10}$$

with

$$\gamma_{eq2,3} = \gamma_{e2}\frac{\gamma_{e2} + \gamma_{eq3,4} - \left(\gamma_{e2} - \gamma_{eq3,4}\right)e^{-2|d_2-d_1|\gamma_{e2}}}{\gamma_{e2} + \gamma_{eq3,4} + \left(\gamma_{e2} - \gamma_{eq3,4}\right)e^{-2|d_2-d_1|\gamma_{e2}}} \tag{11}$$

$$\gamma_{eq3,4} = \gamma_{e3}\frac{\gamma_{e3} + \gamma_{e4,5} - \left(\gamma_{e3} - \gamma_{e4,5}\right)e^{-2|d_3-d_2|\gamma_{e3}}}{\gamma_{e3} + \gamma_{e4,5} + \left(\gamma_{e3} - \gamma_{e4,5}\right)e^{-2|d_3-d_2|\gamma_{e3}}}$$

$$\vdots$$

$$\gamma_{eqN-1,N} = \gamma_{eN-1}\frac{\gamma_{eN-1} + \gamma_{eN} - \left(\gamma_{eN-1} - \gamma_{eN}\right)e^{-2|d_{N-1}-d_{N-2}|\gamma_{eN-1}}}{\gamma_{eN-1} + \gamma_{eN} + \left(\gamma_{eN-1} - \gamma_{eN}\right)e^{-2|d_{N-1}-d_{N-2}|\gamma_{eN-1}}} \tag{12}$$

and

$$\gamma_{e1} = \sqrt{\gamma_1^2 - \gamma_0^2}\,, \quad \gamma_{e2} = \sqrt{\gamma_2^2 - \gamma_0^2}\,, \quad \gamma_{e3} = \sqrt{\gamma_3^2 - \gamma_0^2} \tag{13}$$

$$\gamma_{eN-1} = \sqrt{\gamma_{N-1}^2 - \gamma_0^2}\,, \quad \gamma_{eN} = \sqrt{\gamma_N^2 - \gamma_0^2} \tag{14}$$

It should be noted that the self-element of $\mathbf{Z_e}$ can be evaluated by adopting $h_i = h_j$ and $y_{ij} = r_i$ or r_j.

III. Frequency Domain Responses

Although EHEM is derived and validated with the exact formulas in [17], it still needs further investigations for the following new aspects in frequency domain.

A. Equivalent propagation constant of earth

The newly developed EHEM is based on the concept of equivalent propagation constant of earth. The characteristics of equivalent propagation constant of earth should be investigated with different real multi-layer earth compositions.

As shown in Fig. 2 to Fig. 5, the absolute value of the equivalent propagation constant of earth is calculated based on different earth cases which are given in the Appendix.

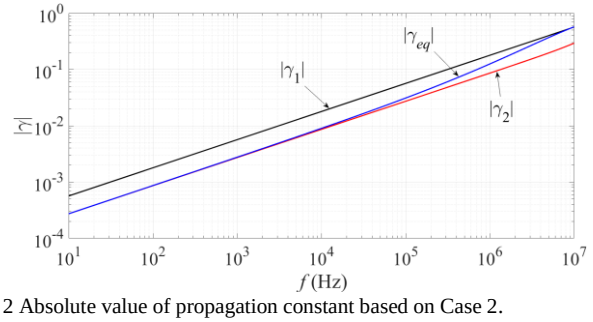

Fig. 2 Absolute value of propagation constant based on Case 2.

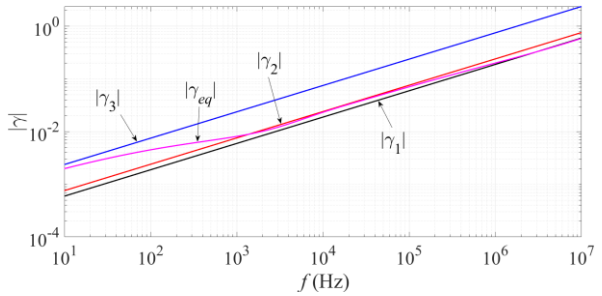

Fig. 3 Absolute value of propagation constant based on Case 5.

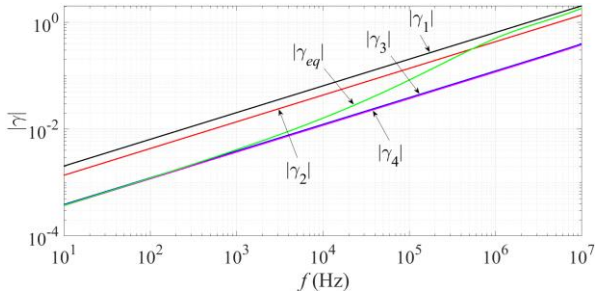

Fig. 4 Absolute value of propagation constant based on Case 8.

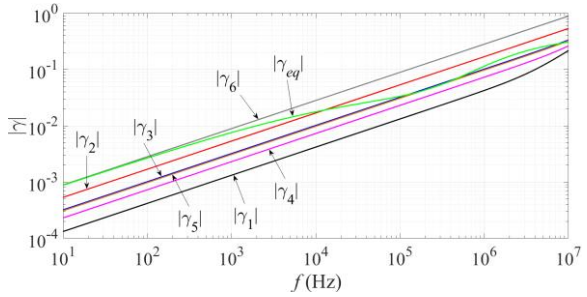

Fig. 5 Absolute value of propagation constant based on Model 19 in [17].

It is clear that $|\gamma_{eq}|$ shows a highly frequency-dependent characteristic. At the low frequency region, $|\gamma_{eq}|$ is the same as the absolute value of propagation constant of earth in the bottom layer, i.e. $|\gamma_{eq}|=|\gamma_2|$ for Case 2 and $|\gamma_{eq}|=|\gamma_3|$ for Case 5. The reason is that the penetration depth of earth is large in the low frequency region, thus the bottom layer is dominated in the calculation of (9) and (10).

However, $|\gamma_{eq}|$ experiences a transition state as frequency increases. Since the penetration depth of earth decreases as frequency increases, $|\gamma_{eq}|$ gradually converges to the absolute value of propagation constant in the upper layers of earth. Therefore, the frequency-dependent transition state of $|\gamma_{eq}|$ is significant in the calculation of earth-return impedance considering influence of multi-layer earth. Moreover, $|\gamma_{eq}|$ shows more complicated transition state in Fig. 5 than those shown in cases 2, 5 and 8 due to more layers of earth. Thus, the transition state can be regarded as a change of dominated layer of earth due to influence of frequency.

B. Comparison of convergence of integrand between exact formula and EHEM

This section mainly discusses the convergence of the integrand used in EHEM, i.e. (4) and (9). The calculated real and imaginary parts of the integrand based on EHEM are compared with the values evaluated using EF formulas (4) and (5). Also, the deviation of the integrand between EHEM and exact formula are explained.

As illustrated in Fig. 6 to Fig. 11, the integrands of mutual impedance based on a three-phase untransposed horizontal overhead line [27] are calculated and analyzed. The line data is h = 25 m, y = 14 m, conductor radius r_c = 1 cm and conductor resistivity ρ_c = 3.78×10^{-8} Ωm. Two frequencies 60 Hz and 100 kHz are adopted into the calculations. Moreover, the real multi-layer earth compositions ranging from two layers to six layers are used in the following evaluations.

A stable convergence of both real and imaginary parts of integrand at f = 60 Hz is observed in Fig. 6, Fig. 8 and Fig. 10. The upper limit of integral variable can be set to 0.1 since the integrand converges effectively to 0. Also, minor differences are observed between EF and EHEM methods in Case 5 and Case 6.

Next, once frequency increases to 100 kHz, the real and imaginary parts of integrand show good convergence as illustrated in Fig. 7, Fig. 9 and Fig. 11. The upper limit of integral variable at high frequency shifts to 1 instead of 0.1 at low frequency. Therefore, it could be straightforward to set the upper limit of integral variable in (4) equal to 1 for EF and EHEM methods, and it is qualitatively enough for accuracy considering a wideband frequency characteristic. Also, the value of both parts of integrand decreases as frequency increases. Again, no significant differences between results evaluated by EF and EHEM are observed.

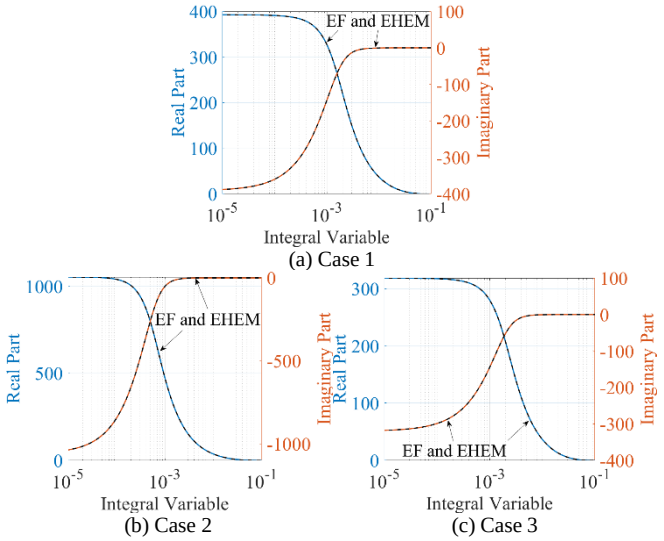

Fig. 6 Real and imaginary parts of integrand evaluated based on EF and EHEM, f = 60 Hz and two layers of earth.

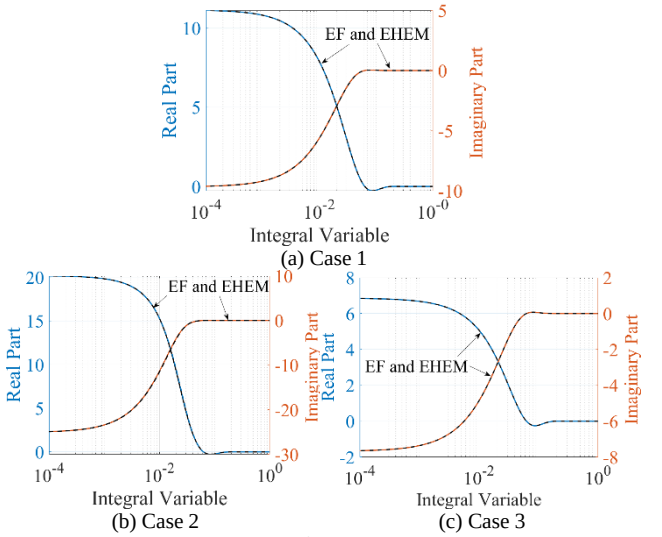

Fig. 7 Real and imaginary parts of integrand evaluated based on EF and EHEM, f = 100 kHz and two layers of earth.

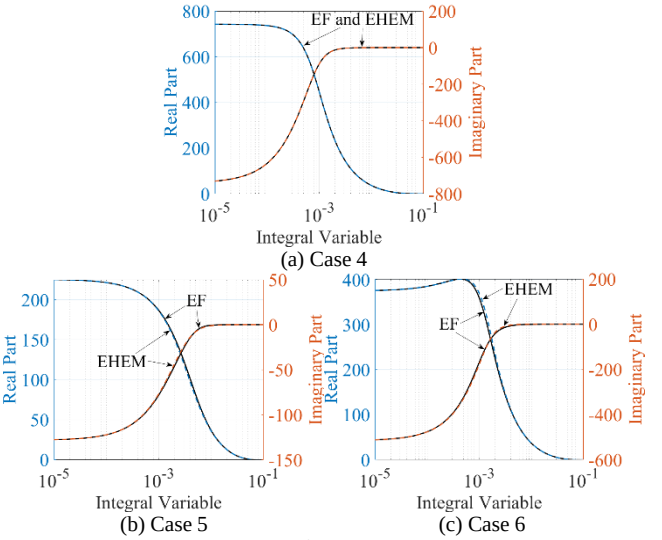

Fig. 8 Real and imaginary parts of integrand evaluated based on EF and EHEM, f = 60 Hz and three layers of earth.

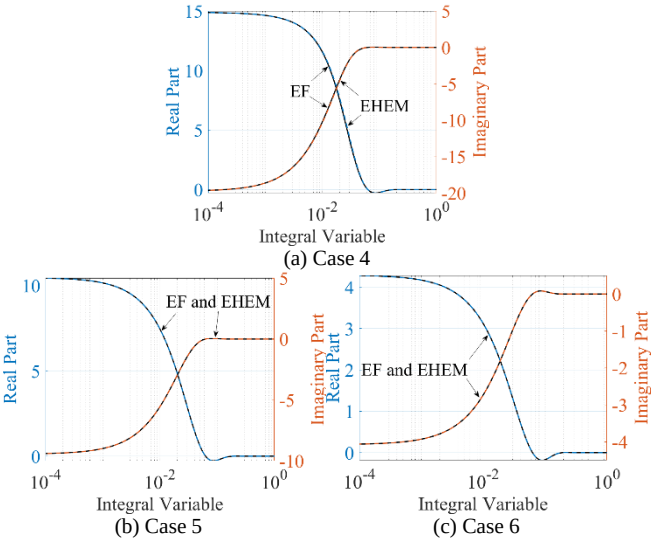

Fig. 9 Real and imaginary parts of integrand evaluated based on EF and EHEM, f = 100 kHz and three layers of earth.

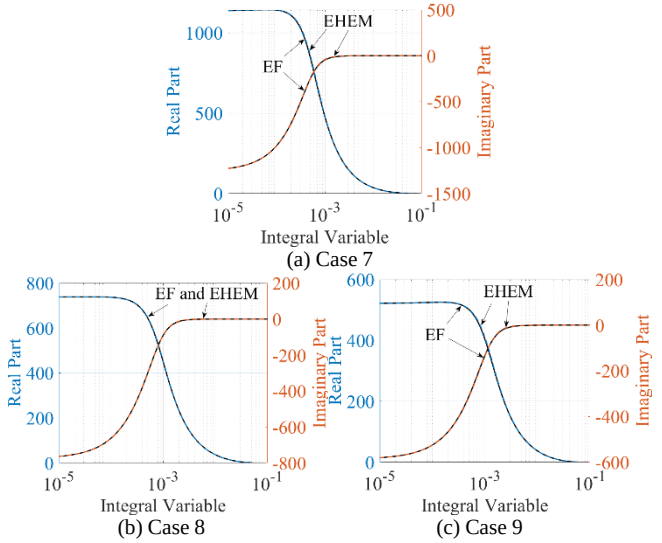

Fig. 10 Real and imaginary parts of integrand evaluated based on EF and EHEM, f = 60 Hz and four layers of earth.

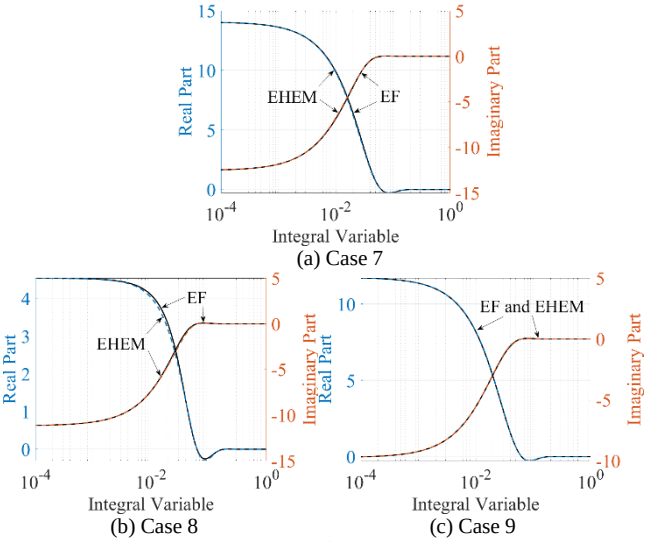

Fig. 11 Real and imaginary parts of integrand evaluated based on EF and EHEM, f = 100 kHz and four layers of earth.

From the view point of impedance calculation, in general, a positive real part of integrand results into a positive reactance of earth-return impedance in (4), and a negative imaginary part of integrand produces a positive resistance of earth-return impedance in (4). Thus, the integrand of EHEM used in (4) shows a high accuracy.

C. Parametric study of EF and EHEM

This section further investigates the parametric influence on calculations of self- and mutual earth-return impedance of overhead lines above a multi-layer earth using EF and EHEM methods. This analysis gives a solid validation of EHEM, which has not been performed in [17].

1) Self-impedance

A single overhead conductor above a multi-layer earth with radius r_c = 1 cm and conductor resistivity $\rho_c = 3.78\times10^{-8}$ Ωm is adopted into the calculations of self-impedance. The deviation is calculated based on (15) and plotted as a function of frequency and height of conductor. The height is varied from 1

m up to 100 m which can cover major vertical configuration of overhead lines.

$$\text{Deviation} = \left| \frac{Z_{11(\text{EHEM})} - Z_{11(\text{EF})}}{Z_{11(\text{EF})}} \right| \times 100\% \qquad (15)$$

where $Z_{11(\text{EHEM})}$ is self-impedance evaluated by (9) and $Z_{11(\text{EF})}$ is self-impedance evaluated by (5).

As illustrated in Fig. 12, Fig. 13 and Fig. 14, the maximum deviations are less than 1% for all cases of earth composition. The visible deviation appears at the high frequency together with conductor close to surface of earth, because EHEM may not represent full characteristics of earth-return effect in high frequency due to its approximation.

In general, the conductor height and earth compositions have negligible influence on deviation of self-impedance.

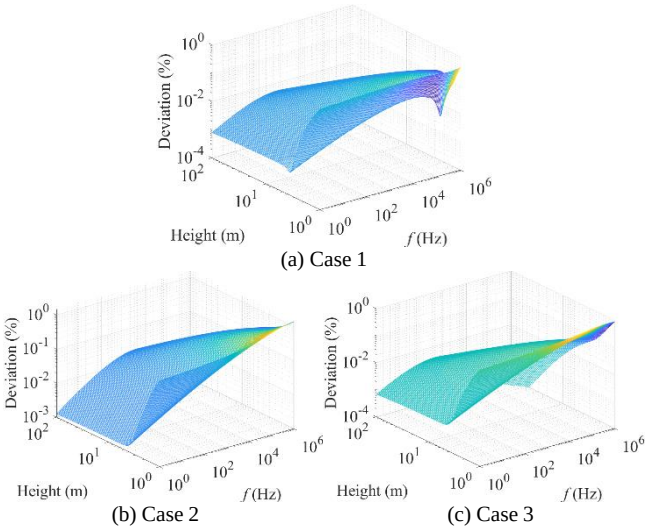

(a) Case 1

(b) Case 2 (c) Case 3

Fig. 12 Deviation of self-impedance as function of height and frequency, two layers of earth.

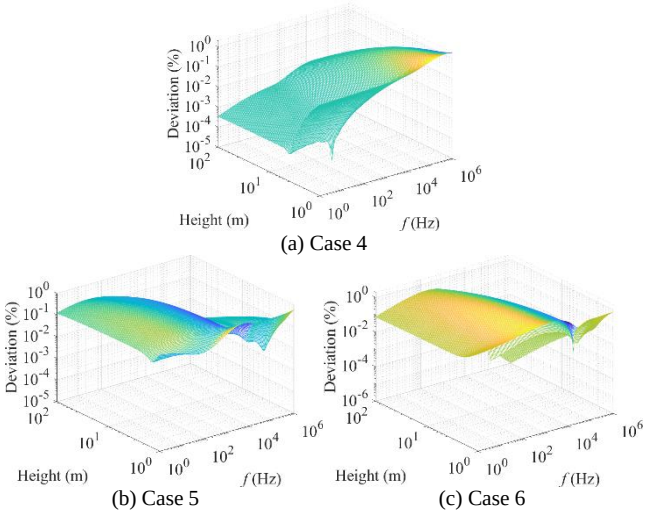

(a) Case 4

(b) Case 5 (c) Case 6

Fig. 13 Deviation of self-impedance as function of height and frequency, three layers of earth.

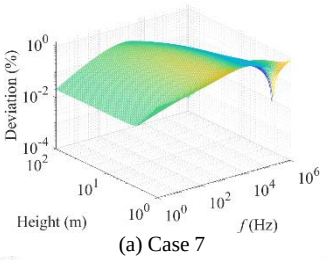

(a) Case 7

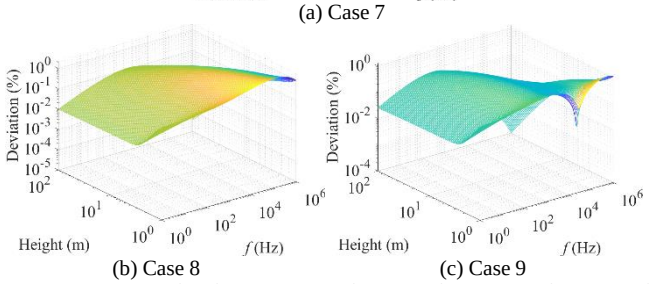

(b) Case 8 (c) Case 9

Fig. 14 Deviation of self-impedance as function of height and frequency, four layers of earth.

2) Mutual impedance

Two overhead conductors above multi-layer earth are adopted into calculations in this section based on vertical and horizontal variations. The deviation of mutual impedance between the conductors are given below.

$$\text{Deviation} = \left| \frac{Z_{12(\text{EHEM})} - Z_{12(\text{EF})}}{Z_{12(\text{EF})}} \right| \times 100\% \qquad (16)$$

where $Z_{12(\text{EHEM})}$ is mutual impedance evaluated by (9) and $Z_{12(\text{EF})}$ is mutual impedance evaluated by (5).

Again, the deviation is calculated as a function of frequency and geometrical configuration.

a) Vertical distance variation

The height of an overhead conductor is set to $h_1 = 25$ m, and the height of another conductor is varied from 1 m to 100 m using logarithmic sampling. The separation between two conductors is $y_{12} = 14$ m.

The deviations evaluated using (16) are shown in Fig. 15, Fig. 16 and Fig. 17. The maximum deviation, i.e. 5%, is observed in Case 6 with large separation and high frequency. In fact, it means that the EHEM is less accurate to represent the complex transition state between multiple layers of earth. A similar phenomenon can be observed in Case 5, Case 7, Case 8 and Case 9. However, the first layer of earth is dominant in very high frequency region, i.e. $f > 100$ kHz, thus, the deviation decreases as frequency increases.

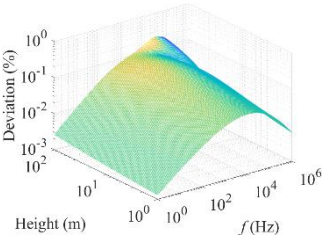

(a) Case 1

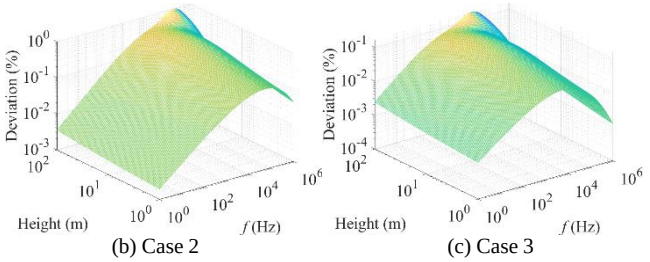

(b) Case 2 (c) Case 3

Fig. 15 Deviation of mutual impedance as function of height and frequency, two layers of earth.

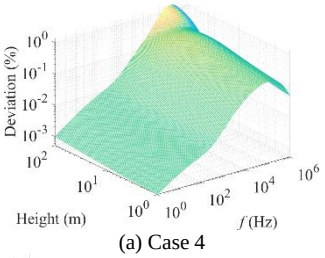

(a) Case 4

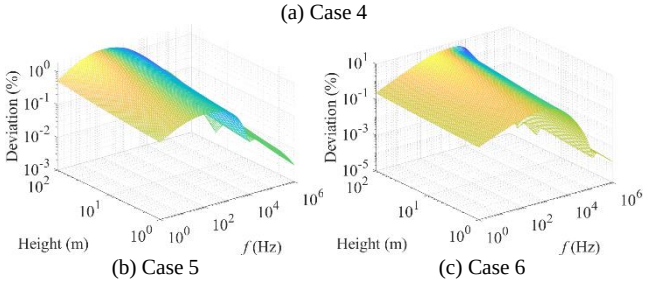

(b) Case 5 (c) Case 6

Fig. 16 Deviation of mutual impedance as function of height and frequency, three layers of earth.

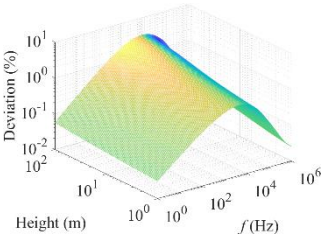

(a) Case 7

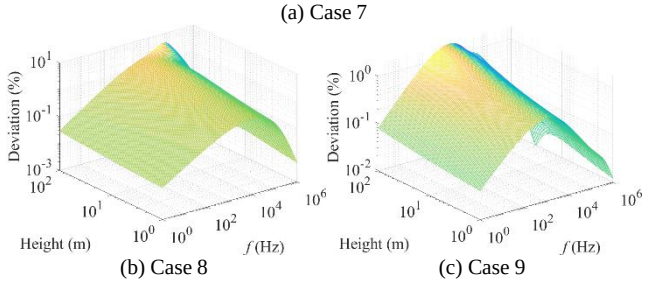

(b) Case 8 (c) Case 9

Fig. 17 Deviation of mutual impedance as function of height and frequency, four layers of earth.

The deviation of mutual impedance is more sensitive to the separation in comparison to results obtained for self-impedance.

b) Horizontal distance variation

The heights of two horizontal overhead conductors are set to $h_1 = h_2 = 25$ m. The separation between two conductors is varied from 1 m to 100 m using logarithmic sampling.

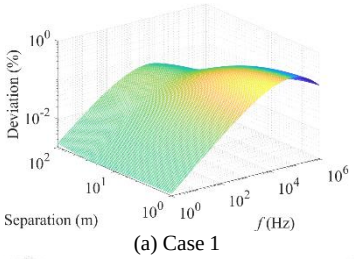

(a) Case 1

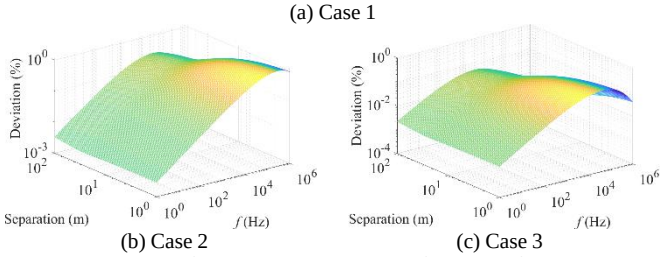

(b) Case 2 (c) Case 3

Fig. 18 Deviation of mutual impedance as function of separation and frequency, two layers of earth.

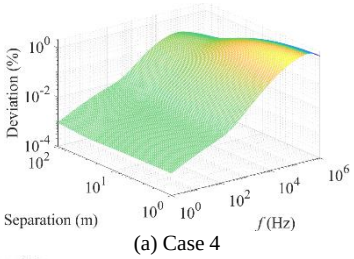

(a) Case 4

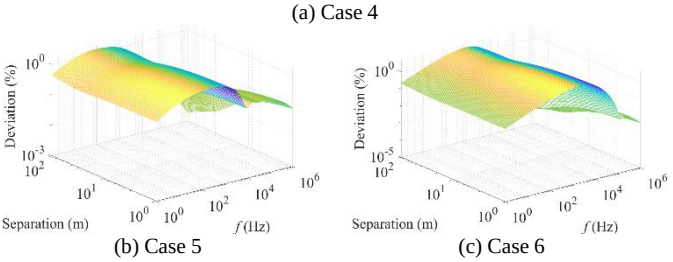

(b) Case 5 (c) Case 6

Fig. 19 Deviation of mutual impedance as function of separation and frequency, three layers of earth.

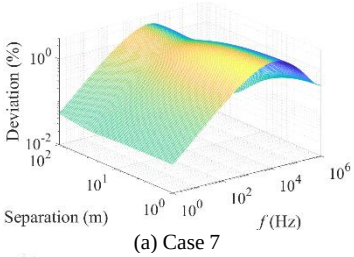

(a) Case 7

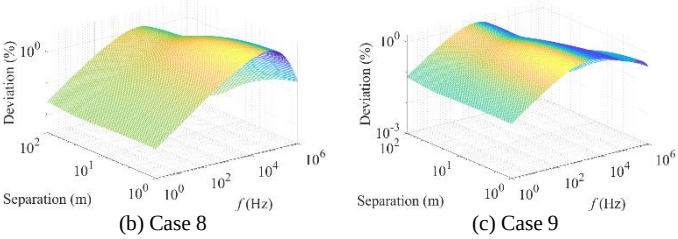

(b) Case 8 (c) Case 9

Fig. 20 Deviation of mutual impedance as function of separation and frequency, four layers of earth.

The maximum deviation is observed in Case 7 with around 2%. It should be noted that the maximum separation is 100 m, and it is much smaller than wavelength 299.79 m at f = 1 MHz.

It should be noted that the earth compositions with five and six layers shown in [17] are also used to validate EHEM against EF method. In general, the deviations of self- and mutual earth-return impedances are less than 5%, although the results are not discussed in this paper.

IV. Conclusions

This paper reviews the recently developed EHEM and EF methods for calculation of earth-return impedance of overhead lines above a multi-layer earth. It presents a comprehensive study of EHEM with the following conclusions.

The characteristics of equivalent propagation constant of earth are highly frequency-dependent. A transition state from low frequency to high frequency is observed, which means that the dominant layer of earth moves from bottom to top as the frequency increases.

The analysis of integrand of EHEM shows high convergence and less errors in comparison to EF method. The deviation of calculation of earth-return impedance is less than 5% in general. Also, it is sensitive to the transverse geometrical dimensions of lines, especially for the height and separation distance of conductors. Therefore, the EHEM can be used in EMT simulations as an important supplement to the EF method.

V. Appendix

The multi-layer earth compositions used in the calculations of Section III are given in Table I [17].

TABLE I
MULTI-LAYER EARTH COMPOSITIONS

Case	Depth of Layers (m)			Resistivity (Ωm)			
	d_1	d_2	d_3	ρ_1	ρ_2	ρ_3	ρ_4
C1	2.7	∞		373	145	-	
C2	2.1			247	1064		
C3	1.7			57	97		
C4	3.1	18.1	∞	128	1923	521	-
C5	3.4	121.8		222	137	14	
C6	1.1	22.2		33	26	284	
C7	1.2	6.5	27.6	235	3571	205	1515
C8	0.3	2.7	7.3	19	42	524	571
C9	4.5	12.5	35.2	122	835	75	334

VI. References

[1] A. Ametani, H. Xue, T. Ohno and H. Khalilnezhad, *Electromagnetic Transients in Large HV Cable Networks: Modeling and Calculations*, IET, 2021.

[2] J. He, R. Zeng, and B. Zhang, *Methodology and Technology for Power System Grounding*. Singapore: John Wiley & Sons Singapore. Ltd., 2013.

[3] L. M. Wedepohl and R. G. Wasley, "Wave propagation in multiconductor overhead lines - Calculation of series impedance for multilayer earth," *Proc. IEE*, vol. 113, pp. 627-632, 1966.

[4] E. D. Sunde, *Earth conduction effects in transmission systems*, New York: Dover, 1968.

[5] M. Nakagawa, A. Ametani, and K. Iwamoto, "Further studies on wave propagation in overhead lines with earth return: Impedance of Stratified Earth," *Proc. IEE*, vol. 120, pp. 1521-1528, 1973.

[6] A. Ametani and R. Schinzinger, "Equations for surge impedance and propagation constant of transmission lines above stratified earth," *IEEE Trans. PAS*, vol. PAS-95 pp. 773-781, 1976.

[7] A. Ametani, "Stratified earth effects on wave propagation-frequency dependent parameters, "*IEEE Trans. PAS*, vol. PAS-93, pp.1233-1239, 1974.

[8] I. S. Moghram, "Effects of earth stratification on impedances of power transmission lines," *Eur. Trans. Elect. Power*, vol. 8, pp. 445-449, 1998.

[9] G. K. Papagiannis, D. A. Tsiamitros, D. P. Labridis, and P. S. Dokopoulos, "A systematic approach to the evaluation of the influence of multi-layered earth on overhead power transmission lines," *IEEE Trans. Power Del.*, vol. 20, no. 4, pp. 2594-2601, 2005.

[10] D. A. Tsiamitros, G. C. Christoforidis, G. K.Papagiannis, D. P. Labridis, and P. S. Dokopoulos, "Earth conduction effects in systems of overhead and underground conductors in multi-layered soils," *IET Proc. Generation, Transmission, Distrib.*, vol. 153, no. 3, pp. 291-299, 2006.

[11] D. A. Tsiamitros, G. K. Papagiannis, and P. S. Dokopoulos, "Earth return impedances of conductor arrangements in multi-layer soils-Part I: Theoretical model," *IEEE Trans. Power Del.*, vol. 23, pp.2392-2400, 2008.

[12] D. A. Tsiamitros, G. K. Papagiannis, and P. S. Dokopoulos, "Earth return impedances of conductor arrangements in multi-layer soils-Part II: Numerical results," *IEEE Trans. Power Del.*, vol. 23, pp.2401-2408. 2008.

[13] A. Ametani, N. Nagaoka, R. Koide, "Wave propagation characteristics on an overhead conductor above snow," *Trans. Inst. Electr. Eng. Jpn*., vol. 134, pp. 26-33, 2001.

[14] T. A. Papadopoulos, G. K. Papagiannis and D. P. Labridis, "A generalized model for the calculation of the impedances and admittances of overhead power lines above stratified earth," *Electric Power Systems Research*, vol. 80, pp. 1160-1170, 2010.

[15] D. A. Tsiamitros, G. K. Papagiannis, and P. S. Dokopoulos, "Homogenous earth approximation of two-layer earth structures: An equivalent resistivity approach," *IEEE Trans. Power Del.*, vol. 22, pp. 658-666, 2007.

[16] A. G. Martins-Britto, F. V. Lopes and S. R. M. J. Rondineau, "Multi-layer earth structure approximation by a homogeneous conductivity soil for ground return impedance calculations," *IEEE Trans. Power Del.*, vol. 35, pp. 881-891, 2020.

[17] H. Xue, J. Mahseredjian, A. Ametani, J. Morales and I. Kocar, "Generalized formulation and surge analysis on overhead lines: impedance / admittance of a multi-layer earth," *IEEE Trans. Power Delivery*, vol. 36, no. 6, pp. 3834-3845, 2021.

[18] H. Xue, A. Ametani, J. Mahseredjian, Y. Baba, F. Rachidi and I. Kocar, "Transient Responses of Overhead Cables due to Mode Transition in High Frequencies", *IEEE Trans. Electromag. Compat*, vol. 60, no. 3, pp.785-794, 2018.

[19] H. Xue, A. Ametani, J. Mahseredjian, Y. Baba and F. Rachidi, "Frequency response of electric and magnetic fields of overhead conductors with particular reference to axial electric field," *IEEE Trans. Electromag. Compat*, vol. 60, no. 6, pp. 2029-2032, 2018.

[20] H. Xue, A. Ametani, J. Mahseredjian and I. Kocar, "Generalized formulation of earth-return impedance / admittance and surge analysis on underground cables," *IEEE Trans. Power Delivery*, vol. 33, no.6, pp.2654-2663, 2018.

[21] H. Xue, A. Ametani, J. Mahseredjian, I. Kocar, "Computation of overhead line / underground cable parameters with improved MoM-SO method," Power Systems Computation Conference (PSCC), Dublin, Ireland, 2018.

[22] H. Xue, A. Ametani and J. Mahseredjian, "Very fast transients in a 500 kV gas - insulated substation," *IEEE Trans. Power Delivery*, vol. 34, no. 2, pp. 627-637, 2019.

[23] H. Xue, A. Ametani and K. Yamamoto, "Theoretical and NEC calculations of electromagnetic fields generated from a multi-phase underground cable," *IEEE Trans. Power Delivery*, vol. 36, no.3, pp.1270-1280, 2021.

[24] H. Xue, A. Ametani and K. Yamamoto, "A study on external electromagnetic characteristics of underground cables with consideration of terminations," *IEEE Trans. Power Delivery*, vol. 36, no. 5, pp. 3255-3265, 2021.

[25] H. Xue, J. Mahseredjian, J. Morales, I. Kocar and A. Xemard, "An investigation of electromagnetic transients for a mixed transmission system with overhead lines and buried cables," *IEEE Trans. Power Delivery*, DOI: 10.1109/TPWRD.2022.3151749, 2022.

[26] H. Xue, J. Mahseredjian, J. Morales and I. Kocar, "Analysis of cross-bonded cables using accurate model parameters," *IEEE Trans. Power Delivery*, DOI: 10.1109/TPWRD.2022.3179832.

[27] A. Ametani, T. Ohno and N. Nagaoka, *Cable System Transients: Theory, Modeling and Simulation*, Wiley-IEEE Press, 2015.